Acta Cryst. (1964). **17**, 434

A Comparison of ω and 2θ Scans for Integrated Intensity Measurement

By R. D. Burbank

Bell Telephone Laboratories, Incorporated, Murray Hill, New Jersey, U.S.A.

(*Received* 20 *December* 1962 *and in revised form* 16 *May* 1963)

To maintain intensity measurements on a fixed scale an identical and constant spectral distribution must be integrated in either the ω or 2θ scan. Both the vertical and horizontal dimensions of the detector aperture are critical for either scan. With the mechanical arrangements currently in use for upper level ω scans both aperture dimensions are dependent on the mosaic spread of the crystal as well as the spectral dispersion. The optimum type of scan for a given set of conditions is that which yields the true integrated intensity plus the least amount of thermal diffuse scattering. This will be the scan which defines the smallest illuminated volume in reciprocal space. When other factors, such as anomalous dispersion, are equal, a long characteristic wavelength is desirable in that it will give rise to a smaller illuminated volume at a given point in reciprocal space than will a short wavelength.

Introduction

The definition of an integrated intensity depends on the experimental technique. The technique under consideration in this paper is that of the small crystal bathed in an incident beam of X-rays in such a fashion that every point on the crystal can see every point on the X-ray source. Under these conditions the integrated intensity (on a relative scale) is defined as a measurement of all the Bragg reflected radiation that is produced when a crystal is rotated sufficiently through the reflecting position, at a uniform angular velocity, for all the mosaic blocks in all parts of the crystal to have the opportunity to diffract some specified spectral distribution from all parts of the source. By this definition an integrated intensity is dependent on the size of the crystal in contrast to the classical technique where a large flat crystal intercepts the entire X-ray beam. The spectral distribution must be specified because if a series of measurements are to be on a common scale the same incident energy spectrum must be used for all measurements.

The requirements for valid integrations under the above definition have been considered in great detail by Furnas (1957). A more elegant treatment in terms of convolutions has been given by Alexander & Smith (1962). In both cases the emphasis was on the Eulerian-cradle geometry of the single-crystal orienter or three-circle goniometer. Alexander & Smith clearly demonstrated that any method which presumes an equivalence of peak height and peak area has an extremely limited range of validity. Only two rotating crystal techniques will be considered here. The 2θ scan, or moving crystal–moving counter scan, where the detector and crystal table have a 2:1 angular coupling, is confined to the zero level and consequently is associated with Eulerian-cradle geometry. The ω scan, or moving crystal-stationary counter scan, is used for both zero and upper levels and is commonly associated with equi-inclination Weissenberg geometry.

The intent of the present paper is to indicate certain similarities and differences which exist between the ω and 2θ scans which have either not been emphasized or not been considered in the previous treatments.

2θ scans and zero level ω scans

Fig. 1 is a geometric representation in reciprocal space of the physical interaction between X-rays and matter that occurs in the course of rotating a crystal through a reflection on the zero level. The notation is that used by Furnas (1957). $\Delta\theta$ is the spectral distribution or wavelength band to be included in the measurement, expressed as an increment of Bragg angle. S is the source width expressed as the angle subtended at the crystal. C is the crystal diameter expressed as the angle subtended at the source. M is the angular width of the mosaic spread. The origin of reciprocal space is at O. The crystal rotation axis is normal to the plane of the figure. A reciprocal lattice point P and a vector OP lie in the plane of the figure. The short wavelength limit of the spectral distribution is defined by a sphere of radius λ_1^{-1} centered at the point S_1. The long wavelength limit is defined by a sphere of radius λ_2^{-1} centered at the point S_2. The incident beam vectors form a sheaf with an angular width $C+S$ and converge at O. The directions of these vectors range from $(C+S)/2$ to $-(C+S)/2$. The points S_1 and S_2 are spread out into arcs and each point on the arcs defines the center of a sphere. A continuum of spheres is defined and the extrema and mean positions of the spheres are indicated in Fig. 1 for the limiting wavelengths. To account for the mosaic spread the point P is replaced by a spherical cap of diameter M. The intersection of the cap with the horizontal plane is indicated in Fig. 1 by a short heavy arc of length M. The crystal is rotated counterclockwise during an integration. The measurement starts when M first touches the sphere of radius λ_1^{-1} oriented at $-(C+S)/2$, forming the vector 1.

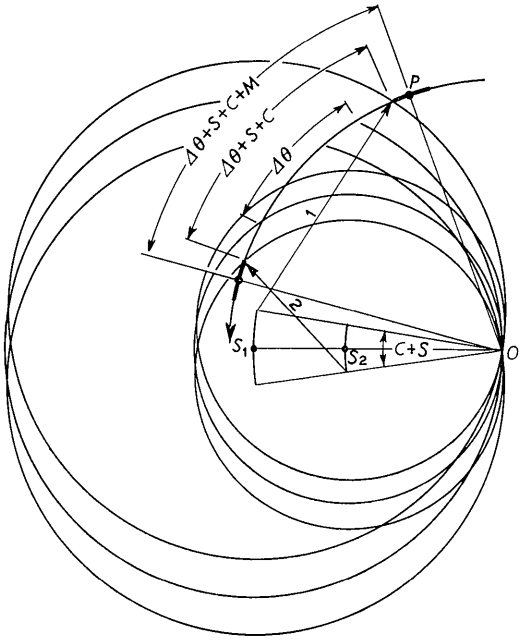

Fig. 1. Representation in reciprocal space of the physical interaction between an X-ray spectral distribution from a finite-sized source and a real crystal on rotation through the reflecting position.

The measurement ends when M last touches the sphere of radius λ_2^{-1} oriented at $+(C+S)/2$, forming the vector 2. Quite clearly the crystal must be rotated through the angle $\Delta\theta+S+C+M$ in the course of the integration.

To find the minimum aperture widths that will accept all the Bragg reflected rays for either the ω or 2θ scans consider Fig. 2. S_1 represents the center of a sphere of radius λ_1^{-1} and it also represents the center of the spectrometer circle. Let vector 1 represent Bragg reflection from a sphere of radius λ_1^{-1} oriented at $-(C+S)/2$. If this ray had originated at the center of the crystal it would intercept the spectrometer circle at the angle $2\theta_1-(C+S)/2$ as indicated by vector 2. However, the sphere oriented at $-(C+S)/2$ is defined by a vector describing an incident ray that passes from $-S/2$ on the source to $+C/2$ on the crystal. Therefore the origin of the diffracted ray is at a point $C/2$ off the center of the spectrometer. As indicated by vector 3 the diffracted ray intercepts the spectrometer circle at a lower angle than vector 2. Thus to accept the interaction represented by vector 1 the detector aperture must be able to accept a ray which intercepts the spectrometer circle at

$$\begin{aligned}2\theta_1-(C+S)/2-(C/2)\cos\,[2\theta_1-(C+S)/2]\\ \simeq 2\theta_1-S/2-(C/2)(1+\cos 2\theta_1)\\ =2\theta_1-S/2-C\cos^2\theta_1\,.\end{aligned}$$

In the 2θ scan the integration starts with the detector centered at $2\theta_1-(S+C+M)$, diffracted ray at $2\theta_1-S/2-C\cos^2\theta_1$, and ends with the detector at $2\theta_2+S+C+M$, diffracted ray at $2\theta_2+S/2+C\cos^2\theta_2$. The detector aperture must have a width from the center of $(2\theta_1-S/2-C\cos^2\theta_1)-[2\theta_1-(S+C+M)]$ on the high angle side and a width from the center of $(2\theta_2+S+C+M)-(2\theta_2+S/2+C\cos^2\theta_2)$ on the low angle side. The sum of the two widths is

$$\begin{aligned}T_h&=S_h+C_h(\sin^2\theta_1+\sin^2\theta_2)+2M\\ &\simeq S_h+2C_h\sin^2\theta_0+2M\end{aligned}\qquad(1)$$

where we have added the subscript h to indicate that we are dealing with horizontal dimensions, and θ_1 and θ_2 are replaced by θ_0 the Bragg angle of the peak intensity at the center of the wavelength band.

In the ω scan the detector is centered at $2\theta_0$ throughout the integration. The detector aperture must have a width from center of $(2\theta_2+S/2+C\cos^2\theta_2)-2\theta_0$ on the high angle side and a width from center of $2\theta_0-(2\theta_1+S/2+C\cos^2\theta_1)$ on the low angle side. The sum of the two widths is

$$\begin{aligned}T_h&=2\theta_2-2\theta_1+S+C(\cos^2\theta_1+\cos^2\theta_2)\\ &\simeq\Delta 2\theta+S_h+2C_h\cos^2\theta_0\end{aligned}\qquad(2)$$

It should be noted in passing that there are several ways of treating the effect of crystal size as it enters into equations (1) and (2) (Furnas, 1957; Burbank, 1962; Ladell & Spielberg, 1963; Alexander & Smith, 1964).* They differ as to the degree of geometric approximation that is used to define the origin point of a diffracted beam vector. They all agree on several points:

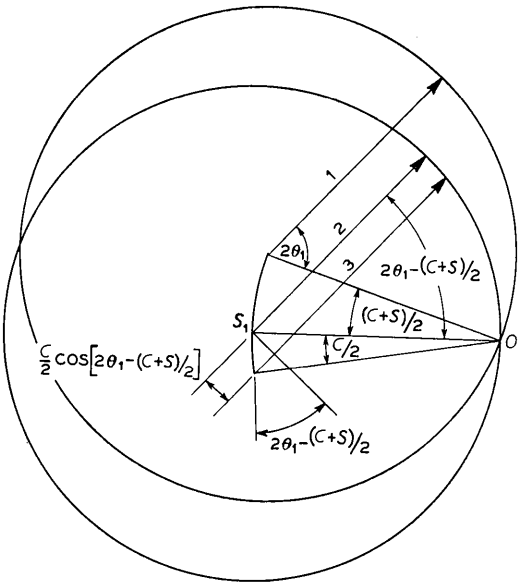

Fig. 2. Displacement of the origin of a diffracted beam vector arising from combined size effect of source and crystal.

* *Note added in proof.*— It should be noted that the crystal size effect in equations (1) and (2) is identical with that derived by Alexander & Smith (1962) in their first paper.

1. For the 2θ scan the effect is zero at $\theta=0°$ and has a maximum of $2C$ at $\theta=90°$.
2. For the ω scan the effect has a maximum of $2C$ at $\theta=0°$ and is zero at $\theta=90°$.
3. At $\theta=45°$ the effect is identical for either scan.

For all practical purposes the differences that remain are of little consequence.

The minimum aperture height that will accept all the Bragg reflected rays for either the ω or 2θ scan is apparent upon consideration of the third dimension in Fig. 1, normal to the plane of the paper. The sheaf of incident beam vectors has an angular divergence of S_v+C_v in the vertical direction and the spherical cap of the mosaic spread has a height M. The necessary aperture is

$$T_v=S_v+C_v+M\ . \qquad (3)$$

It is a curious consequence of the natural spectral distribution of an X-ray emission line that the definition of the quantity $\Delta 2\theta$ is entirely arbitrary unless the spectral distribution is defined by balanced filters. It is well known that the shape of the distribution approximates that of a Cauchy distribution (Ladell, Parrish & Taylor, 1959). Furnas has used the separation of the $K\alpha_1$–$K\alpha_2$ doublet plus the widths at half maximum intensity of the $K\alpha_1$ and $K\alpha_2$ lines to define $\Delta 2\theta$. This will include 85% of the area under the calculated Cauchy distribution of a doublet. Alexander & Smith have suggested using the separation of the doublet plus 2·5 times the widths at half maximum of the lines. The writer has used the separation of the doublet plus 3·15 times the widths at half maximum of the lines for comparative computations of minimum apertures. This includes 95% of the area under the calculated Cauchy distribution. Once $\Delta 2\theta$ is defined the scanning ranges and minimum apertures should consistently conform to the definition or a variable scale factor will enter into the results*.

If the balanced filter technique is used $\Delta 2\theta$ is defined by the difference in wavelength of the absorption edges of the filters. An advantage of the technique is that it can be used with the 2θ scan for a direct determination of the mosaic spread. Equations (1) and (3) show that this quantity is needed for all techniques. Recall that with balanced filters a reflection is always measured as a pair of curves. The curves diverge at the point where any wavelength in the pass band can enter the detector. The curves converge again at the point where no wavelength in the pass band can enter the detector. From Fig. 1 it is obvious that the curves first diverge when the detector is at $2\theta_1-(S+C+M)$, and converge again when the detector is at $2\theta_2+(S+C+M)$. The positions of θ_1 and θ_2 are known from the peak position and a direct measure of $S+C+M$ is obtained. The method is best applied to a strong reflection at low Bragg angle where the Lorentz polarization effect is large, dispersion is small, and the divergence or convergence of the curves is most visible.

Equations (1), (2) and (3) provide the simplest comparison of the ω and 2θ scans. In the 2θ scan the horizontal dimension of the detector aperture is independent of dispersion, but does depend on the mosaic spread, and has a definite upper limit for a given X-ray source and crystal. For a zero level ω scan the horizontal aperture is independent of mosaic spread, but does depend on dispersion and consequently has no upper limit. In both scans the vertical aperture depends on the mosaic spread. The simplest practical consequence is that a single aperture may be adequate for 2θ scans but a series of apertures may be required for the ω scan. A small aperture area is desirable for several reasons. A small aperture will collect less unwanted scattering from all sources, such as parasitic scattering, Compton scattering, *etc.* Most of the contribution of unwanted scattering to an intensity measurement can be eliminated by proper background corrections. The principal disadvantage is a reduction of the signal to noise ratio with a consequent increase in the error of counting statistics and in the minimum observable intensity.

A more fundamental reason for minimizing aperture areas is related to an inherent limitation in all intensity measurements. The effect of thermal diffuse scattering is to produce a peak coincident with the Bragg peak, which tails off slowly at the sides. Under ideal conditions a measured intensity will consist of the true integrated intensity plus some contribution from TDS. Nilsson (1957) has shown that some of the published measurements on potassium chloride and sodium chloride may be in error by 20 to 30% from TDS. As the volume of reciprocal space from which diffraction can be detected at a given moment is reduced, the amount of TDS that will be incorporated in an integration is reduced. Therefore the proper way to compare the effects of aperture requirements on intensities would appear to be in terms of illuminated volumes in reciprocal space (by definition an illuminated volume is the volume of reciprocal space from which diffraction can be detected).

To obtain an estimate of the illuminated volume consider Fig. 3. The origin of reciprocal space is at O. S_0O represents an incident beam vector $\mathbf{s}_0\lambda^{-1}$ passing from the center of the source to the center of the crystal. S_0T_0 represents a diffracted beam vector $\mathbf{s}\lambda^{-1}$ passing from the center of the crystal to the center of the detector. OT_0 therefore represents a diffraction vector $(\mathbf{s}-\mathbf{s}_0)\lambda^{-1}$ and the point T_0 is an illuminated

* *Note added July* 15, 1963, *in reply to point raised by referee.* In this paragraph and subsequently we speak of $\Delta 2\theta$ being defined by a fraction of a Cauchy distribution. This is a simplification for convenience. It is not implied that there is a 1 to 1 correspondence between an area under a Cauchy distribution and an area under a reflection peak. The correspondence will vary from reflection to reflection because of the convolutive nature of an intensity peak. There is nothing in this paragraph that tells *how* one can experimentally conform to the definition of $\Delta 2\theta$ if balanced filters are not used.

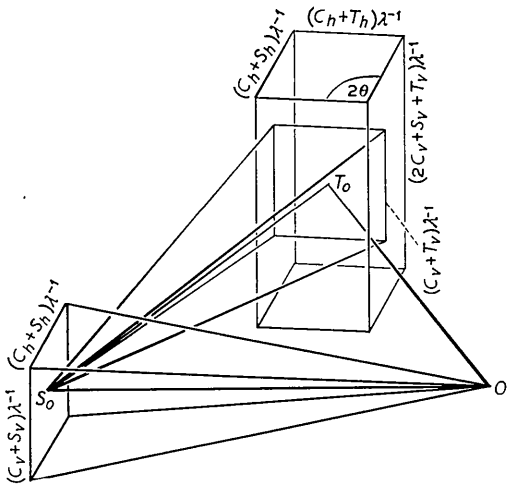

Fig. 3. Illuminated volume in reciprocal space formed by diffracted beam vector sheaves originating at every point in incident beam vector sheaf.

point in reciprocal space. An array of all possible illuminated points will sweep out a volume, the illuminated volume for the wavelength considered. Let the maximum horizontal and vertical angular dimensions of crystal, source, and detector be C_h, C_v, S_h, S_v, T_h and T_v. Then the incident beam is represented by a sheaf of $\mathbf{s}_0\lambda^{-1}$ vectors which converge at O. The base of the sheaf has the linear dimensions $(C_h+S_h)\lambda^{-1}$ by $(C_v+S_v)\lambda^{-1}$. All the diffracted rays will be accepted by the detector which are defined by a sheaf of $\mathbf{s}\lambda^{-1}$ vectors of angular dimensions (C_h+T_h) by (C_v+T_v) which diverge from the starting point of any $\mathbf{s}_0\lambda^{-1}$ vector. In Fig. 3 a single sheaf of $\mathbf{s}\lambda^{-1}$ vectors is shown diverging from the point S_0. The base of the sheaf has the linear dimensions $(C_h+T_h)\lambda^{-1}$ by $(C_v+T_v)\lambda^{-1}$. Now let a sheaf of $\mathbf{s}\lambda^{-1}$ vectors originate at every starting point in the $\mathbf{s}_0\lambda^{-1}$ sheaf. An evelope of $\mathbf{s}\lambda^{-1}$ sheaves results which defines the illuminated volume illustrated in Fig. 3. This quantity is related to the dimensions of the experiment by the expression

$$V=\lambda^{-3}(2C_v+S_v+T_v)(C_h+S_h)(C_h+T_h)\sin 2\theta \quad (4)$$

where T_h and T_v are given by equations (1), (2) and (3). The prismatic parallelogram is an excellent approximation even for circular apertures and a variety of crystal shapes as long as C_h, C_v, T_h and T_v refer to maximum dimensions in the horizontal and vertical directions. The prismatic parallelogram will always enclose any volume that might be defined by a higher approximation. It is worth noting that the spherical crystal is the only shape that gives constant values of C_h and C_v for every reflection.

When ω and 2θ scans are compared by the criteria of minimum illuminated volume for a variety of experimental conditions (including values of M up to 0·5°) several conclusions emerge. When using balanced filters the 2θ scan is always indicated. When $\Delta 2\theta$ is defined by some fraction of the Cauchy distribution the 2θ scan is always indicated at sufficiently high Bragg angles but at lower angles the ω scan is indicated if M is large, the 2θ scan if M is small. In actual practice the detector apertures will rarely be as small as the minimum acceptable values of equations (1), (2) and (3), except for the ω scan with balanced filters or at very high angles without balanced filters. Therefore, in general, one will not work with the minimum illuminated volume. Under these circumstances it is worth while to consider the influence of choice of radiation on illuminated volume. For the portion of reciprocal space that is accessible to both Cu and Mo radiation the 2θ scan will require an illuminated volume with Mo that runs from 5 to 10 times as large as with Cu. For the ω scan with balanced filters Mo requires about 1·5 to 2 times the illuminated volume for Cu. For the ω scan with $\Delta 2\theta$ equivalent to 95% of a Cauchy distribution Mo requires 3·5 to 4·5 times the illuminated volume for Cu. A longer wavelength is clearly advantageous if other factors such as anomalous dispersion do not dictate otherwise.

In comparing ω and 2θ scans it is commonly said that in the ω scan a reciprocal lattice point is scanned in a tangential direction while in a 2θ scan a reciprocal lattice point is scanned in a radial direction. As a corollary to this it is further said that one scans along the Laue streak in the 2θ scan and across the Laue streak in the ω scan. It is often forgotten that the first statement applies only to a very special situation where the incident beam is absolutely parallel, the source contains only one wavelength, *i.e.* the spectral distribution has the form of a delta function, the sample is a point crystal with no mosaic spread, and the detector has an infinitely narrow aperture.

In any real case none of these restrictions will apply; the physical interaction which should be included in an integrated intensity measurement occurs when a properly oriented crystal is rotated by a sufficient amount through the reflecting position. This physical interaction is dependent only on rotating the crystal, as shown in Fig. 1. It is in no way dependent on detector motion, detector apertures, or even whether a detector is present at all. If a detector is present, with the correct apertures and motion for the scan involved, an identical signal will be obtained for either the ω or 2θ scan. The unwanted radiation or noise that is included with the signal will generally be different for the two scans. In a valid ω scan exactly the same peak shape and Laue streak will be seen on the intensity curve as in the 2θ scan. The Laue streak will be of limited length only because of the finite aperture. The over-all effect is that the peak comes down to a Laue streak which appears like a pair of shoulders, and these drop down to a residual background. An ω scan curve is thus characterized by three regions. In the central region all Bragg reflected radiation from the crystal is accepted. The intermediate region is a transition region. It begins with all Bragg reflected radiation being accepted and ends with none being

accepted. In the outer region no Bragg reflected radiation is accepted from the crystal. If an inadequate aperture is used with the ω scan the transition region will be lost in the sides of the peak. For all techniques except balanced filters the proper background level occurs in the central region. If the minimum aperture equation (2) is used with balanced filters the limits of the pass band will occur within the transition region (because of the convolutive nature of an intensity curve). With a sufficiently large aperture the limits of the pass band will occur in the central region. Gross errors will result with any technique if a background level is taken in the outer region.

The ω and 2θ scans are compared in Fig. 4 for the special case of parallel radiation incident on a point crystal with no mosaic spread. The spectral distribution to be included in the integration is defined on the short wavelength side by a sphere of radius λ_1^{-1} centered at S_1, on the long wavelength side by a sphere of radius λ_2^{-1} centered at S_2. For the 2θ scan an infinitely narrow aperture will define an illuminated line which extends along the vector OP from $2\lambda_2^{-1}\sin\theta$ to $2\lambda_1^{-1}\sin\theta$. As the scan proceeds from OP at $90°+\theta_1$ to $90°+\theta_2$ the illuminated line moves radially along OP from the initial limits $2\lambda_2^{-1}\sin\theta_1$, $2\lambda_1^{-1}\sin\theta_1$ to the final limits $2\lambda_2^{-1}\sin\theta_2$, $2\lambda_1^{-1}\sin\theta_2$. For the ω scan the detector aperture must extend from $2\theta_1$ to $2\theta_2$ to detect the desired radiation. An illuminated area is defined which is bounded by the initial and final illuminated lines of the 2θ scan and by two circular arcs, one extending from $2\lambda_2^{-1}\sin\theta_1$ to $2\lambda_2^{-1}\sin\theta_2$, the other from $2\lambda_1^{-1}\sin\theta_1$ to $2\lambda_1^{-1}\sin\theta_2$. As the scan proceeds the illuminated area does indeed move tangentially to the vector OP. Note, however, that the illuminated area always includes an illuminated line along OP which is identical with the illuminated line of the 2θ scan.

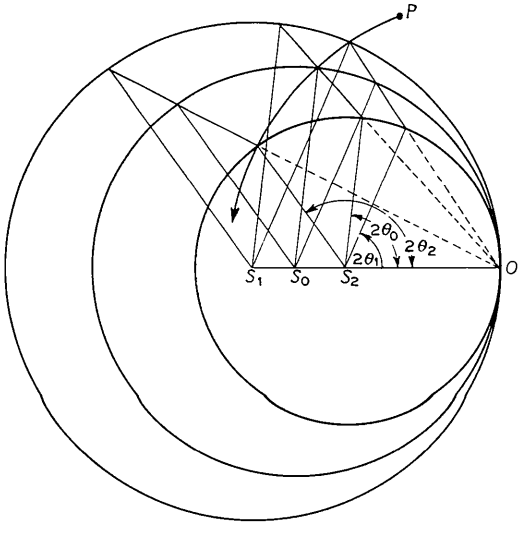

Fig. 4. Diffraction of a real spectral distribution from a point source by a non-mosaic, point crystal. 2θ scan with point detector defines illuminated line along OP with radial motion. ω scan defines illuminated area with tangential motion. The area always contains the illuminated line of the 2θ scan. Construction applies to real source, crystal, and detector upon replacing each illuminated point by an illuminated volume.

Strictly speaking, Fig. 4 applies only to the case of balanced filters. The difference between two scans is taken. What remains is the spectral distribution within the pass band which has definite limits defining λ_1 and λ_2. For other techniques the length of an illuminated line is defined by the voltage on the X-ray tube on the short wavelength side, and by the transparency of all windows in the system and the sensitivity of the detector on the long wavelength side.

When one removes the special conditions of Fig. 4 and considers the interaction between a source of finite size and a real crystal, only one change is necessary. Each illuminated point in Fig. 4 is replaced by an illuminated volume as defined by equation (4).

Upper level ω scans with equi-inclination Weissenberg geometry

Fig. 5 is a schematic illustration in perspective of the equi-inclination Weissenberg geometry. To preserve clarity no spheres of reflection are drawn in. A perfectly parallel incident beam is considered and a point crystal with no mosaic spread. O is the origin of reciprocal space, OO' is the crystal rotation axis. The incident beam direction is parallel to the line S_1O. The spectral distribution is defined on the short wavelength side by a sphere of radius λ_1^{-1} whose center is at S_1, on the long wavelength side by a sphere of radius λ_2^{-1} whose center is at S_2. The wavelength of peak intensity is λ_0. As a crystal is rotated a reciprocal lattice point P moves along the path $P_1P_0P_2$. In standard Weissenberg terminology RSO is the angle μ, QSP is the angle ν, RSQ is the angle Υ, and OSP is

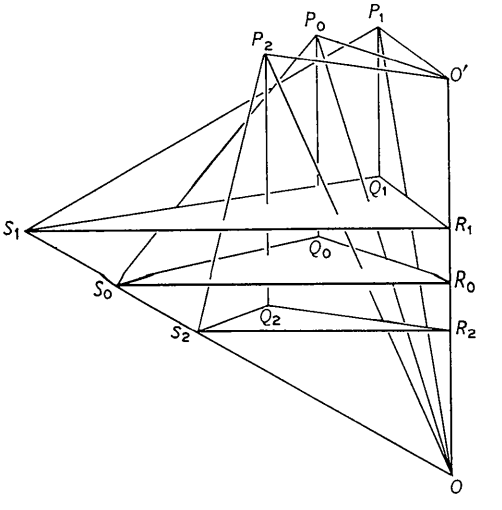

Fig. 5. Diffraction with equi-inclination Weissenberg geometry of a real spectral distribution from a point source by a non-mosaic, point crystal. To preserve clarity no spheres of reflection are depicted.

the angle 2θ. At P_0 the equi-inclination condition holds and the incident and diffracted beams are equally inclined to the rotation axis. The inclination of the incident beam is constant for all wavelengths, but the diffracted beam becomes more and more inclined from S_1P_1 through S_2P_2.

It is quite possible to discuss the spectral dispersion $\Delta 2\theta$ in terms of the instrumental components $\Delta\nu$ and $\Delta\Upsilon$. However, a more penetrating analysis results if attention is focused on the diffraction plane defined by the incident and diffracted beam vectors SO and SP. The intersection of the diffraction plane with the sphere of reflection defines a great circle for a given wavelength. On the zero level the great circle is horizontal and in Fig. 5 it would appear edge on along the line SO. For an upper level a great circle centered at S will pass through the points O and P. The upper level great circle is inclined to the zero level great circle with an intersection along the line SO, *i.e.* the circle has been rotated around the line SO. Let the amount of rotation around the incident beam vector be designated by the angle α. This quantity is fundamental to upper level recording and it is essential to know how it varies as a function of wavelength and reciprocal lattice coordinates.

In Fig. 6 the equi-inclination geometry is reoriented so that the prime reference direction is the incident beam vector SO. Three orthogonal projections are shown. In each case the outer full circle is the projection of a sphere of radius λ^{-1}. A reciprocal lattice point P is defined by axial and radial cylindrical reciprocal lattice coordinates ζ and ξ. In Fig. 6(*c*) the rotation axis OO' and the axial coordinate ζ lie in the plane of the figure, but ξ does not. Only components of OO', ζ and ξ appear in Fig. 6(*a*) and (*b*). In Fig. 6(*a*) the point P intersects the sphere in the great circle defined by S, O, P which is inclined to the plane of the figure by the angle α. If this great circle is rotated about the axis SO by the angle α it will then lie in the plane of the figure and P will move to P'. The angle $OSP = OSP' = 2\theta$. The motion of P to P' lies on a small circle which is perpendicular to the figure. The center of the small circle lies on the line SO and is located $(\cos 2\theta)/\lambda$ to the right of S. The radius of the small circle is $(\sin 2\theta)/\lambda$. In Fig. 6(*b*) the preceding construction is viewed along the direction OS. The horizontal and inclined great circles appear edge on as lines through OP' and OP. The small circle through PP' is parallel to the plane of the figure. The height of P above the horizontal great circle is given by $\sin\alpha(\sin 2\theta)/\lambda$. In Fig. 6(*c*) the construction is viewed along the direction in the horizontal great circle which is perpendicular to SO. The projection of ξ is the line PO' which is perpendicular to OO'. The horizontal and vertical components of OO' are given by $\zeta\sin\mu$ and $\zeta\cos\mu$. The horizontal component of PO' is given by

$$\begin{aligned} PO'\cos\mu &= SO - SP' - \zeta\sin\mu \\ &= \lambda^{-1} - (\cos 2\theta)/\lambda - \zeta\sin\mu\,. \end{aligned}$$

So

$$PO' = (1 - \cos 2\theta - \zeta\lambda\sin\mu)/\lambda\cos\mu\,.$$

The vertical component of PO' is given by

$$PO'\sin\mu = \tan\mu(1 - \cos 2\theta - \zeta\lambda\sin\mu)/\lambda\,.$$

The height of P above the horizontal great circle is thus given by

$$\zeta\cos\mu - \tan\mu(1 - \cos 2\theta - \zeta\lambda\sin\mu)/\lambda\,.$$

Equating the two expressions for the height of P above the horizontal circle

$$\sin\alpha = [\zeta\lambda\cos\mu - \tan\mu(1 - \cos 2\theta - \zeta\lambda\sin\mu)]/\sin 2\theta\,. \tag{5}$$

Let λ_0 be the wavelength of peak intensity in the spectral distribution. The equi-inclination setting is determined by ζ and λ_0 so that

$$\begin{aligned} \sin\mu &= \zeta\lambda_0/2 \\ \cos\mu &= \tfrac{1}{2}\sqrt{(4 - \zeta^2\lambda_0^2)} \\ \tan\mu &= \zeta\lambda_0/\sqrt{(4 - \zeta^2\lambda_0^2)}\,. \end{aligned} \tag{6}$$

The Bragg angle depends upon ζ, ξ and λ which may be any wavelength in the spectral distribution so that

$$\begin{aligned} \sin 2\theta &= \tfrac{1}{2}\sqrt{\{(\zeta^2\lambda^2 + \xi^2\lambda^2)(4 - \zeta^2\lambda^2 - \xi^2\lambda^2)\}} \\ 1 - \cos 2\theta &= \tfrac{1}{2}(\zeta^2\lambda^2 + \xi^2\lambda^2)\,. \end{aligned} \tag{7}$$

Substituting equations (6) and (7) into equation (5)

$$\sin\alpha = \frac{\zeta\lambda(4 - \zeta^2\lambda\lambda_0 - \xi^2\lambda\lambda_0)}{\sqrt{\{(4 - \zeta^2\lambda_0^2)(\zeta^2\lambda^2 + \xi^2\lambda^2)(4 - \zeta^2\lambda^2 - \xi^2\lambda^2)\}}}\,. \tag{8}$$

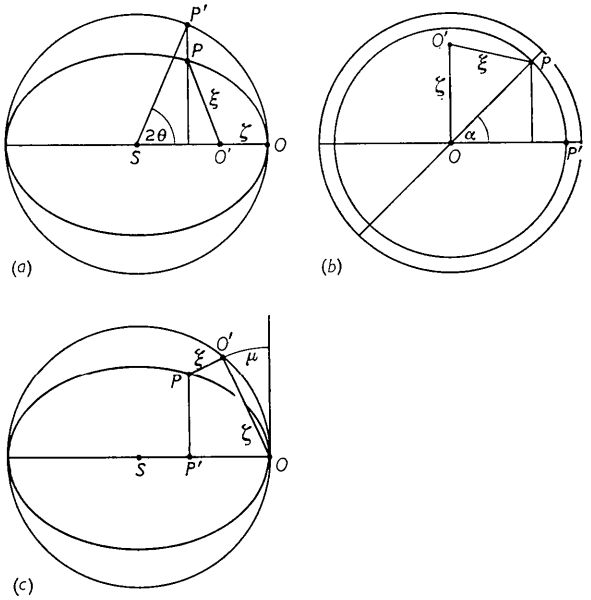

Fig. 6. Equi-inclination geometry. Construction for expressing the inclination, α, of the plane of diffraction as a function of wavelength and the reciprocal lattice coordinates of a point, P.

When $\lambda = \lambda_0$ equation (8) reduces to

$$\sin \alpha = \tan \mu \operatorname{ctn} \theta_0 . \qquad (9)$$

From equation (8) the behavior of α can be detailed. In Table 1 the variation of α as a function of $\zeta\lambda_0$, $\xi\lambda_0$ is presented for values out to the limiting sphere. This is the value of α that will pertain at the peak intensity of a reflection. The value of α changes throughout a reflection and as a point P moves from P_1 to P_2 in Fig. 5 the value of α passes through a minimum at P_0. It is essential to know the extent of this variation. In Table 2 the variation of α between Mo $K\alpha_1$ and the Zr and Y K edges is presented, and in Table 3 the variation of α between Cu $K\alpha_1$ and the Ni and Co K edges. The spectral dispersion of a balanced filter pass band can be considered as the upper limit of dispersion that will be encountered in practice. Therefore Tables 2 and 3 indicate that for all practical purposes α can be considered constant throughout an integration unless a reciprocal lattice point is very close to the limiting sphere or has a value of $\zeta\lambda_0$ which exceeds the limitations of any real apparatus.

The preceding conclusion permits a tremendous simplification in discussing the detector aperture requirements for the upper level ω scan. The geometry of Fig. 1 can be applied directly, just remembering that the frame of reference has been rotated by α around the mean incident beam direction. If the crystal is restricted to a spherical shape and the detector is positioned so that its horizontal and vertical aperture dimensions are parallel and perpendicular to the inclined diffraction plane, then equations (2) and (3) can be written

$$\begin{aligned} T_h^\alpha &= \Delta 2\theta + S_h \cos\alpha + S_v \sin\alpha + 2C\cos^2\theta \\ T_v^\alpha &= S_h \sin\alpha + S_v \cos\alpha + C + M \end{aligned} \qquad (10)$$

remembering that the image of the source is rotated

Table 1. *The inclination, α, of the plane of diffraction as a function of $\zeta\lambda_0$, $\zeta\lambda_0$ for equi-inclination Weissenberg geometry, where λ_0 is the wavelength of peak intensity in the spectral distribution*

$\zeta\lambda_0$	$\xi\lambda_0 \rightarrow$ 0·0	0·2	0·4	0·6	0·8	1·0	1·2	1·4	1·6	1·8	2·0
0·0	—	0·00	0·00	0·00	0·00	0·00	0·00	0·00	0·00	0·00	0·00
0·2	90·00	44·72	25·98	17·55	12·83	9·77	7·53	5·77	4·23	2·70	
0·4	90·00	62·85	43·80	31·87	24·10	18·63	14·48	11·08	8·05	4·92	
0·6	90·00	70·63	54·45	42·17	33·00	25·98	20·35	15·52	11·03	6·02	
0·8	90·00	74·65	60·80	49·10	39·50	31·57	24·80	18·68	12·60	4·40	
1·0	90·00	76·92	64·60	53·55	43·83	35·27	27·50	20·02	11·72		
1·2	90·00	78·15	66·72	56·02	46·10	36·85	27·88	18·37	0·00		
1·4	90·00	78·58	67·38	56·52	46·00	35·52	24·32	8·05			
1·6	90·00	78·07	66·15	54·18	41·82	27·95	0·00				
1·8	90·00	75·33	60·15	43·50	21·30						
2·0	90·00										

Table 2. *Variation of α between* Mo $K\alpha$ *and* Zr *and* Y K *edges**

$\zeta\lambda_0$	$\xi\lambda_0 \rightarrow$ 0·2	0·4	0·6	0·8	1·0	1·2	1·4	1·6	1·8
0·2	0·00	0·00	0·00	0·00	0·00	0·00	0·00	0·00	0·02
	0·00	0·00	0·00	0·00	0·00	0·00	0·00	0·00	0·03
0·4	0·00	0·00	0·01	0·00	0·00	0·00	0·00	0·02	0·05
	0·00	0·02	0·01	0·00	0·00	0·00	0·02	0·02	0·10
0·6	0·02	0·00	0·00	0·02	0·02	0·00	0·01	0·04	0·13
	0·02	0·00	0·00	0·02	0·02	0·02	0·01	0·05	0·41
0·8	0·02	0·00	0·02	0·02	0·01	0·02	0·04	0·08	0·60
	0·03	0·02	0·02	0·02	0·01	0·02	0·04	0·13	†
1·0	0·02	0·03	0·02	0·04	0·03	0·03	0·06	0·21	
	0·05	0·05	0·03	0·04	0·03	0·05	0·10	0·60	
1·2	0·08	0·05	0·05	0·05	0·05	0·10	0·20	5·03	
	0·10	0·06	0·05	0·07	0·07	0·14	0·40	†	
1·4	0·20	0·10	0·10	0·10	0·15	0·26	1·80		
	0·24	0·14	0·11	0·13	0·21	0·66	†		
1·6	0·48	0·30	0·25	0·30	0·57	8·97			
	0·65	0·40	0·37	0·51	1·58	†			
1·8	1·69	1·07	1·18	3·03					
	3·25	2·23	3·90	†					

* The first entry refers to Zr, the second to Y.

† Bragg reflection cannot occur at these points for $\lambda = $ Y K edge.

Table 3. *Variation of α between* Cu $K\alpha_1$ *and* Ni *and* Co K *edges**

$\zeta\lambda_0$	$\xi\lambda_0 \rightarrow$ 0·2	0·4	0·6	0·8	1·0	1·2	1·4	1·6	1·8
0·2	0·00	0·00	0·00	0·00	0·00	0·00	0·00	0·00	0·03
	0·00	0·00	0·00	0·00	0·00	0·02	0·01	0·02	0·12
0·4	0·00	0·02	0·01	0·00	0·00	0·00	0·02	0·02	0·06
	0·00	0·02	0·01	0·00	0·00	0·02	0·04	0·07	0·41
0·6	0·04	0·00	0·00	0·02	0·02	0·02	0·03	0·05	0·18
	0·04	0·02	0·01	0·02	0·04	0·03	0·06	0·15	3·05
0·8	0·03	0·02	0·02	0·02	0·03	0·02	0·05	0·12	0·75
	0·07	0·03	0·03	0·05	0·05	0·07	0·14	0·43	†
1·0	0·05	0·05	0·03	0·04	0·03	0·05	0·10	0·28	
	0·13	0·08	0·07	0·09	0·10	0·13	0·33	3·43	
1·2	0·12	0·06	0·05	0·07	0·08	0·12	0·26	5·50	
	0·18	0·16	0·15	0·17	0·22	0·39	1·58	†	
1·4	0·27	0·15	0·13	0·13	0·20	0·36	2·20		
	0·69	0·39	0·35	0·40	0·65	2·15	†		
1·6	0·66	0·40	0·35	0·41	0·77	9·82			
	2·01	1·17	1·14	1·73	9·17	†			
1·8	2·40	1·45	1·60	3·80					
	†	9·73	†	†					

* The first entry refers to Ni, the second to Co.
† Bragg reflection cannot occur at these points for $\lambda =$ Co K edge.

by α around the incident beam direction, and using the superscript α to indicate the orientation of the detector.

The apertures of equation (10) are somewhat larger than those of equations (2) and (3) because of the contribution of source size. Otherwise the functional dependence is the same. To a first approximation the detector aperture required for a zero level ω scan will suffice for an upper level scan provided the detector is rotated around the mean diffracted beam direction by such an angle that the horizontal and vertical edges of the aperture are parallel and perpendicular, repsectively, to the inclined diffraction plane. Call this angle β. It turns out that β has the same magnitude as α, but this is not obvious immediately. One way of demonstrating that $\beta = \alpha$ is presented in the Appendix.

If the detector is not rotated around the diffracted beam direction the minimum aperture requirements are

$$T_h^0 = T_h^\alpha \cos\alpha + T_v^\alpha \sin\alpha$$
$$T_v^0 = T_h^\alpha \sin\alpha + T_v^\alpha \cos\alpha$$

since the area enclosed by the unrotated detector aperture must enclose the area of the rotated detector aperture. In unfavorable circumstances $T_h^0 \times T_v^0$ may be an order of magnitude larger than $T_h^\alpha \times T_v^\alpha$. Note that T_h^0 and T_v^0 are each dependent on both the mosaic spread and the spectral dispersion. So far as aperture requirements are concerned the zero level ω scan with Eulerian-cradle geometry has distinct advantages over equi-inclination geometry.

An analysis similar to that presented here can be made for any type of upper level geometry. An investigation of normal beam geometry has shown that the functional dependence of α on $\zeta\lambda$ and $\xi\lambda$ is considerably more complicated than for equi-inclination geometry. For practical purposes it seems unlikely that serious consideration need be given any upper level geometry except the equi-inclination case.

APPENDIX

The equality of the angles β and α in the equi-inclination case

The incident and diffracted beam vectors define the plane of diffraction. The intersection of the plane of diffraction with the sphere of reflection defines a great circle. This circle is horizontal for a zero level but is inclined by the angle α around the incident beam direction for an upper level. The incident beam is inclined by the angle μ to the horizontal in the equi-inclination case.

Let the angle β be the amount by which the detector must be rotated around the diffracted beam direction so that the horizontal and vertical edges of the detector aperture are parallel and perpendicular, respectively, to the plane of the inclined great circle.

Place a great circle in the xy plane with its center at the origin of a right handed cartesian coordinate system, and define the angle 2θ as in Fig. 7(a). Let the great circle be given a rotation μ around the x axis as in Fig. 7(b). Follow this by a rotation α around the diameter which lies in the yz plane as in Fig. 7(c). Then the equations of a point on the inclined great circle in parametric form are given by

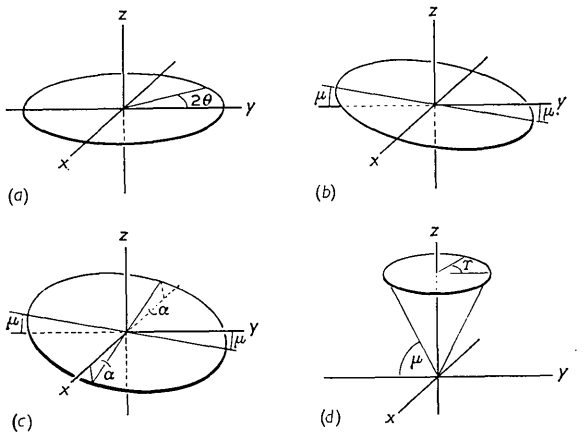

Fig. 7. Equi-inclination geometry. Constructions for determining the angle, β, by which the detector must be rotated around the diffracted beam vector so that the horizontal and vertical edges of the detector aperture are parallel and perpendicular to the inclined plane of diffraction.

$$\begin{aligned} x &= -\sin 2\theta \cos\alpha \\ y &= \cos 2\theta \cos\mu + \sin 2\theta \sin\mu \sin\alpha \\ z &= -\cos 2\theta \sin\mu + \sin 2\theta \cos\mu \sin\alpha \end{aligned} \qquad (11)$$

The same point also lies on the small circle that is traversed by the detector when it is adjusted for the inclination angle μ. Let the small circle be parallel to the xy plane, with its center on the z axis at a height $\sin\mu$ above the xy plane, and define the angle Υ as in Fig. 7(*d*). Then the equations of the point on the small circle in parametric form are given by

$$\begin{aligned} x &= -\sin\Upsilon\cos\mu \\ y &= \cos\Upsilon\cos\mu \\ z &= \sin\mu \end{aligned} \qquad (12)$$

The angle between the tangents to the two circles at the points x, y, z is the angle β. Using the direction cosines of the two curves one obtains

$$\cos\beta = \frac{\frac{dx}{d2\theta}\frac{dx}{d\Upsilon} + \frac{dy}{d2\theta}\frac{dy}{d\Upsilon} + \frac{dz}{d2\theta}\frac{dz}{d\Upsilon}}{\sqrt{\left(\left(\frac{dx}{d2\theta}\right)^2 + \left(\frac{dy}{d2\theta}\right)^2 + \left(\frac{dz}{d2\theta}\right)^2\right)}\sqrt{\left(\left(\frac{dx}{d\Upsilon}\right)^2 + \left(\frac{dy}{d\Upsilon}\right)^2 + \left(\frac{dz}{d\Upsilon}\right)^2\right)}}$$

$$= \cos 2\theta \cos\Upsilon\cos\alpha + \sin 2\theta \sin\Upsilon\cos\mu - \cos 2\theta \sin\Upsilon\sin\mu\sin\alpha . \qquad (13)$$

To show the identity of β and α recall that

$$\sin\alpha = \tan\mu \operatorname{ctn}\theta \qquad (9)$$

from which it follows that

$$\cos\alpha = \sqrt{(\cos^2\mu - \cos^2\theta)}/\cos\mu\sin\theta . \qquad (14)$$

Also for equi-inclination geometry

$$\cos\Upsilon/2 = \cos\theta/\cos\mu$$

from which it follows that

$$\sin\Upsilon = 2\cos\theta\sqrt{(\cos^2\mu - \cos^2\theta)}/\cos^2\mu \qquad (15)$$

$$\cos\Upsilon = (2\cos^2\theta - \cos^2\mu)/\cos^2\mu . \qquad (16)$$

When equations (9), (14), (15) and (16) are substituted in equation (13) along with

$$\begin{aligned} \cos 2\theta &= 2\cos^2\theta - 1 \\ \sin 2\theta &= 2\sin\theta\cos\theta \end{aligned}$$

one obtains

$$\cos\beta = \sqrt{(\cos^2\mu - \cos^2\theta)}/\cos\mu\sin\theta = \cos\alpha ,$$

or $\beta = \alpha$.

I am indebted to S. C. Abrahams for many stimulating discussions on methods of integrated intensity measurement.

References

ALEXANDER, L. E. & SMITH, G. S. (1962). *Acta Cryst.* **15**, 983.

ALEXANDER, L. E. & SMITH, G. S. (1964). *Acta Cryst.* In the press.

BURBANK, R. D. (1962). Unpublished first draft of the present paper.*

FURNAS, T. C. (1957). *Single Crystal Orienter Instruction Manual.* Milwaukee: General Electric Company.

LADELL, J., PARRISH, W. & TAYLOR, J. (1959). *Acta Cryst.* **12**, 561.

LADELL, J. & SPIELBERG, N. (1963). *Acta Cryst.*, **16**, 1057.

NILSSON, N. (1957). *Ark. Fys.* **12**, 247.

* This contains a derivation of the crystal size effect for a point source and spherical crystal. The result for the 2θ scan is $2C\sin\theta$, for the ω scan $2C\cos\theta$.